HHS Public Access

Author manuscript

J Mol Biol. Author manuscript; available in PMC 2021 February 14.

Published in final edited form as:

J Mol Biol. 2020 February 14; 432(4): 1297–1304. doi:10.1016/j.jmb.2019.12.009.

Demonstration that small molecules can bind and stabilize low-abundance short-lived RNA excited conformational states

Laura R. Ganser[a], **Megan L. Kelly**[a], **Neeraj N. Patwardhan**[b], **Amanda E. Hargrove**[a,b], **Hashim M. Al-Hashimi**[a,*]

[a]Department of Biochemistry, Duke University Medical Center, Durham, NC, 27710, USA

[b]Department of Chemistry, Duke University, Durham, NC, 27708, USA

Abstract

Many promising RNA drug targets have functions that require the formation of RNA-protein complexes, but inhibiting RNA-protein interactions can prove difficult using small molecules. Regulatory RNAs have been shown to transiently form excited conformational states (ESs) that remodel local aspects of secondary structure. In some cases, the ES conformation has been shown to be inactive and to be poorly recognized by protein binding partners. In these cases, specifically targeting and stabilizing the RNA ES using a small molecule provides a rational structure-based strategy for inhibiting RNA activity. However, this requires that a small molecule discriminate between two conformations of the same RNA to preferentially bind and stabilize the short-lived low-abundance ES relative to the longer-lived more abundant ground state (GS). Here, we tested the feasibility of this approach by designing a mutant that inverts the conformational equilibrium of the HIV-1 transactivation response element (TAR) RNA such that the native GS conformation becomes a low-abundance ES. Using this mutant and NMR chemical shift mapping experiments, we show that argininamide, a ligand mimic of TAR's cognate protein binding partner Tat, is able to restore a native-like conformation by preferentially binding and stabilizing the transient and low-populated ES. A synthetic small molecule optimized to bind the TAR GS also partially stabilized the ES whereas an aminoglycoside molecule that binds RNAs non-specifically did not preferentially stabilize the ES to a similar extent. These results support the feasibility of inhibiting RNA activity using small molecules that preferentially bind and stabilize the ES.

Graphical Abstract

*Correspondence to: hashim.al.hashimi@duke.edu; Tel: 919-660-1113.

Author Contributions

Laura R. Ganser: Conceptualization, Methodology, Investigation, Visualizaiton, Writing-Original draft, and Writing- Reviewing and editing. **Megan L. Kelly:** Investigation and Writing-Reviewing and editing. **Neeraj N. Patwardhan**: Resources and Writing-Reviewing and editing. **Amanda E. Hargrove**: Resources and Writing- Reviewing and editing. **Hashim M. Al-Hashimi**: Conceptualization, Methodology, Writing- Original draft, Writing- Reviewing and editing, and Supervision.

Declaration of Interest

H.M.A.–H is an advisor to and holds an ownership interest in Nymirum Inc, an RNA-based drug discovery company.

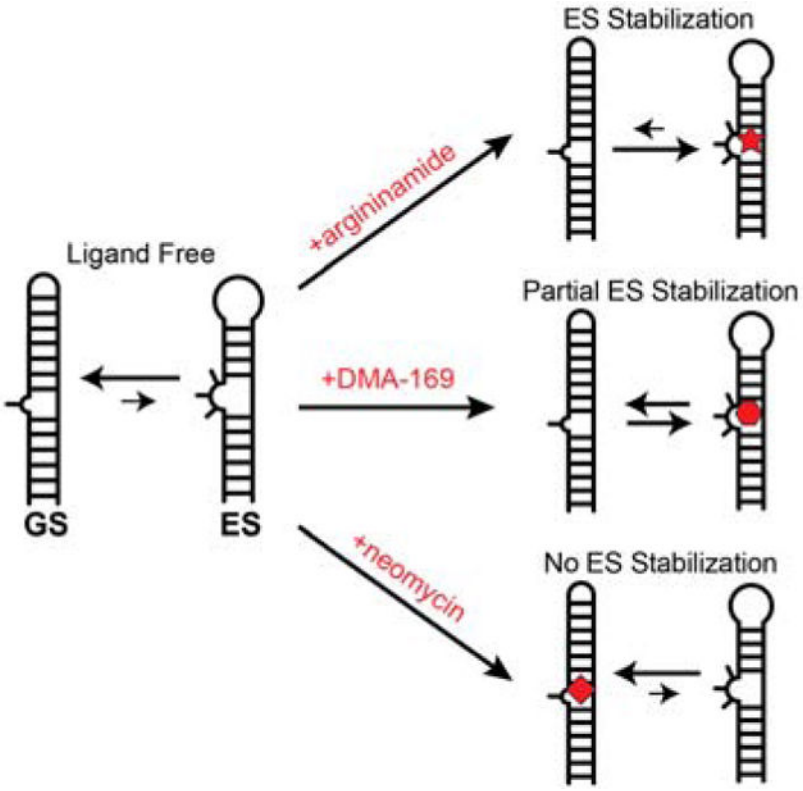

Keywords

RNA dynamics; HIV-1; TAR; ensemble; drug discovery

Although RNA is increasingly recognized to be an attractive target in drug discovery efforts [1–5], identifying small molecules that can bind to RNA specifically and inhibit cellular activity remains challenging. One of the only proven strategies for therapeutically targeting RNAs is to disrupt their structural dynamics [6–9]. This can prevent RNAs from adopting their active conformation or prevent transitions between multiple conformations required to execute multi-step biochemical reactions. Indeed, several antibiotics function by impairing the structural dynamics of ribosomal RNA [8, 9]. A similar approach could potentially be used to inhibit RNA-protein interactions, which prove difficult to inhibit using small molecules given their large interaction interface [10, 11].

Many regulatory RNAs form alternative short-lived (lifetimes typically lower than milliseconds) and low-populated (populations typically <10%) conformations often referred to as ‘excited states’ (ES) that change base pairing in and around non-canonical motifs such as bulges and loops [12–15]. These alternative conformations have been shown to play important roles as intermediates that help break up RNA secondary structural transitions into multiple facile steps [12, 16] or that drive conformational adaptation of riboswitches during ligand recognition [17, 18].

A few RNA drug targets whose functions rely on binding to protein partners, including the HIV-1 transactivation response element (TAR) [12, 13, 19, 20] and the Rev response element (RRE) [21, 22] have been shown to form ESs that as of yet do not have any known functions. These ESs are inactive because they can no longer bind their cognate protein binding partners due to their altered secondary structure [22, 23]. We have proposed that targeting and stabilizing ESs with small molecules may provide a new route to inhibit RNA activity [12, 13, 22, 23]. However, it remains to be established whether or not a small molecule can discriminate between two alternative conformations of the same RNA target to preferentially stabilize the short-lived low-abundance ES.

To test whether or not a small molecule can invert an RNA conformational equilibrium by stabilizing the minor ES, we took advantage of the highly studied HIV-1 TAR RNA [10, 24–26]. Wild-type TAR (wtTAR) has been shown to adopt an ES that dramatically alters its secondary structure [13, 27], reshuffling base pairs in the bulge, upper stem, and apical loop resulting in a structure that is enriched in non-canonical mispairs (Fig 1a). Since many small molecules are known that bind the ground state (GS) secondary structure of TAR [24, 28, 29] but none that bind to the alternative ES, we adopted a “reverse-engineering” strategy and designed a TAR mutant ($TAR^{UUCG\text{-}ES}$ mutant, Fig 1a) [27, 30] that inverts the conformational equilibrium so that the ES conformation of wtTAR now becomes the dominant GS conformation in the mutant whereas the wtTAR GS now becomes a low-abundance and short-lived ES in the $TAR^{UUCG\text{-}ES}$ mutant (Fig 1a). We then asked whether ligands known to bind the wtTAR GS can bind to the $TAR^{UUCG\text{-}ES}$ mutant and restore the native GS conformation by binding and preferentially stabilizing its ES.

We previously validated the secondary structure of the $TAR^{UUCG\text{-}ES}$ mutant using NOE distance-based connectivity and chemical shift analysis [27, 30] (Fig 1a) and demonstrated that it stabilizes the native TAR ES as the dominant conformation based on the agreement between the chemical shifts observed for the mutant and those measured for the ES using NMR measurements of spin relaxation in the rotating frame ($R_{1\rho}$)[31–34]. We hypothesized that $TAR^{UUCG\text{-}ES}$ would back exchange with a minor ES conformation that resembles the native GS conformation of wtTAR; in other words, the mutation would invert the conformational equilibrium. Mutants that stabilize ESs of proteins [35] and DNA [36] have been shown to back exchange with GS-like conformations. In addition, based on its sequence, the $TAR^{UUCG\text{-}ES}$ mutant is predicted to adopt an ES conformation that is similar to the wtTAR GS [37](Supplementary Fig 1).

To test whether the $TAR^{UUCG\text{-}ES}$ mutant back exchanges with a GS-like conformation, we measured on- and off-resonance $R_{1\rho}$ relaxation dispersion (RD) on residue-type (G, C, A, U) specifically $^{13}C/^{15}N$ labeled [27] $TAR^{UUCG\text{-}ES}$ (Fig 1b). $R_{1\rho}$ RD profiles consistent with chemical exchange on the micro-to-millisecond timescales were observed at A22, U23, and A35 all of which are expected to undergo a conformational change if $TAR^{UUCG\text{-}ES}$ were to back exchange with a GS-like conformation (Fig 1b). In addition, we observed RD for resonances in the UUCG apical loop (U51-C1’, U52-C6, C53-C1’, C53-C6, and G54-C1’), which was used to stabilize the ES, but which is expected to undergo a conformational change if the mutant were to back exchange with a GS-like conformation (Fig 1 and Supplemental Fig 2). This is interesting because cUUCGg is a highly stable motif and does

not show any sign of chemical exchange in the wtTAR sequence context [38]. The lack of exchange in the latter case can be explained by the fact that replacing the wtTAR apical loop with UUCG also removes sequence elements required for formation of the ES. As a negative control, we did not observe RD for G43-C8, which is not expected to undergo a conformational change when forming a GS-like conformation (Fig 1b).

The RD data could be globally combined and satisfactorily fit to a two-state exchange model sharing the population (p_{ES} ~ 12.6 ±1.0%) and rate of exchange ($k_{ex} = k_1 + k_{-1}$ ~ 173 ±17 s^{-1}) as expected for a concerted secondary structural rearrangement (Fig 1 and Supplementary Tables 1 and 2). As expected, the differences between the ES and GS chemical shifts ($\Delta\omega = \omega_{ES} - \omega_{GS}$) measured for A22-C1' ($\Delta\omega$ = 2.26±0.08) and U23-C6 ($\Delta\omega$ = −2.57±0.07) in $TAR^{UUCG\text{-}ES}$ are of similar magnitude but opposite direction relative to the corresponding differences measured for wtTAR using $R_{1\rho}$ ($\Delta\omega$ = −2.2±0.05 and 2.3±0.1 respectively, Fig 1c)[13]. Thus, the chemical shifts of the $TAR^{UUCG\text{-}ES}$ ES are similar to those of the wtTAR GS (Fig 1c). While the ES chemical shift for A35-C8 is downfield shifted ($\Delta\omega$ = 5.22±0.09) as expected based on the GS of wtTAR, the magnitude of the change is larger than would be observed for the GS of wtTAR ($\Delta\omega$ = −2.4±0.04)[13]. However, this is not surprising considering that this nucleotide is in the apical loop (Fig 1a), and it is likely that the $TAR^{UUCG\text{-}ES}$ ES apical loop containing UUCG will have different structural and/or dynamic properties relative to the wtTAR GS apical loop conformation.

Based on the slow/intermediate exchange kinetics (k_{ex} ~173 s^{-1}) and relatively high population (~12.6%) (Supplementary Table 2), we expect to observe minor resonances for the ES in 2D [^{13}C, ^{1}H] SOFAST-HMQC NMR spectra of $TAR^{UUCG\text{-}ES}$ [39]. Indeed, we did observe minor resonances that have chemical shifts that are in very good agreement with the ES chemical shifts measured for U23-C6 and A35-C8 in $TAR^{UUCG\text{-}ES}$ using $R_{1\rho}$ as well as additional resonances that are in good agreement with the chemical shifts measured for wtTAR, providing additional evidence for back exchange into a GS-like conformation in the $TAR^{UUCG\text{-}ES}$ mutant (Supplementary Fig 3). These results highlight the robustness of the RNA dynamic landscape [40, 41]; even the large modification used to generate $TAR^{UUCG\text{-}ES}$ preserves the GS and ES as the main conformations that undergo micro-to-millisecond chemical exchange detectable by $R_{1\rho}$ RD.

Having established that $TAR^{UUCG\text{-}ES}$ back exchanges into an ES that has structural characteristics of the native wtTAR GS, we next asked whether molecules known to bind the wtTAR GS could preferentially bind, and thereby stabilize, the low populated and short-lived ES of $TAR^{UUCG\text{-}ES}$. For this to occur, the small molecule would have to preferentially bind to the wtTAR GS relative to the ES and to use differences in binding energy to tip the equilibrium in favor of the ES. Argininamide (ARG) serves as a mimetic of TAR's cognate protein partner Tat and has been shown to bind wtTAR in the bulge and induce a unique base triple conformation [19, 20, 24, 42] (Fig 2a).

We used NMR chemical shift titrations to examine whether ARG can invert the equilibrium and preferentially bind and stabilize the ES of $TAR^{UUCG\text{-}ES}$ (Fig 2b). The incremental addition of ARG up to 3.2 mM to $^{13}C/^{15}N$ labeled $TAR^{UUCG\text{-}ES}$ (50 μM) resulted in large chemical shift perturbations for many nucleotides that are directed toward the chemical

shifts of the wtTAR-ARG complex (Fig 2b and Supplementary Fig 4). Line broadening observed at low ARG concentrations indicates that binding of ARG to $TAR^{UUCG\text{-}ES}$ occurs on the intermediate/slow NMR timescale (Supplementary Fig 4) whereas it is in fast exchange for a TAR variant containing a UUCG apical loop [42](Orlovsky *et al* submitted). This may reflect slower on rates in the case of $TAR^{UUCG\text{-}ES}$ given the slow inter-conversion between the “inactive” GS and “active” ES. Indeed, such slow NMR exchange kinetics due to slower apparent on rates were previously reported for binding of theophylline to its RNA aptamer [43]. Although the 2D [^{13}C, ^{1}H] aromatic SOFAST-HMQC [39] of the $TAR^{UUCG\text{-}ES}$ differ markedly from those of wtTAR, those of the $TAR^{UUCG\text{-}ES}$-ARG complex are in very good agreement with their wtTAR-ARG complex counterpart (Fig 2b). Small differences in chemical shifts are observed that may reflect slight differences in the conformation or dynamics of the two constructs (Fig 2b). These results show that ARG can bind the $TAR^{UUCG\text{-}ES}$ and restore native wtTAR conformation by preferentially stabilizing a low-abundance short-lived ES.

To examine whether a synthetic small molecule could also preferentially bind and stabilize an RNA ES, we tested a dimethyl amiloride derivative, DMA-169, which was previously designed to optimally bind wtTAR with high affinity and specificity [44] (Fig 3a and Supplementary Fig 4). We initially confirmed that DMA-169 does indeed preferentially bind the wtTAR in the GS conformation by asking whether or not the NMR spectra of wtTAR measured in the presence of DMA-169 changes when using a TAR mutant that destabilizes the ES relative to the GS ($TAR^{UUCG\text{-}GS}$)[13](Supplementary Fig 5). The excellent agreement confirms that DMA-169 does indeed predominantly bind to the wtTAR GS (Supplementary Fig 5). NMR titrations show that binding of DMA-169 to $TAR^{UUCG\text{-}ES}$ is slow on the NMR chemical shift timescale (Fig 3a and Supplementary Fig 4), while it binds wtTAR in fast exchange [44] (Supplementary Fig 4). Again, this likely reflects differences in the binding pathways and a slow transition toward the ES in either the free or ligand-bound $TAR^{UUCG\text{-}ES}$. While NMR spectra show that DMA-169 does not fully invert the equilibrium to the wtTAR GS bound conformation, the ES is partially stabilized as evidenced by the appearance of minor resonances that are in slow exchange on the NMR timescale and that have chemical shifts that are in very good agreement with chemical shifts observed for the wtTAR-DMA-169 complex (Fig 3a). Due to the limited solubility of DMA-169, it was not possible to saturate binding.

As a negative control, we tested neomycin, which is an aminoglycoside bearing five positively charged ammonium groups that binds wtTAR [45], but that is also known to bind a variety of RNA conformations in part driven by non-specific electrostatic interactions [46] (Fig 3b). Based on 2D [^{13}C, ^{1}H] SOFAST-HMQC spectra [39] neomycin does indeed bind $TAR^{UUCG\text{-}ES}$ (Fig 3b and Supplementary Fig 4). For some resonances in the bulge (U23, C24, U25), the chemical shift perturbations are directed toward spectra of the wtTAR-neomycin complex although none show exact overlap [26, 47](Supplementary Fig 6). Other resonances (G26 and A22) show clear deviations [26, 47](Fig 3b). For A22 the deviations could arise from differences between the wtTAR GS and $TAR^{UUCG\text{-}ES}$ ES apical loop, as replacing the wtTAR apical loop with UUCG ($TAR^{UUCG\text{-}GS}$) also causes chemical shift deviations at A22 in the presence of neomycin (Supplementary Fig 5). These results indicate that neomycin could bind the ES of $TAR^{UUCG\text{-}ES}$ but leaves open the possibility for binding

to conformations other than the native wtTAR GS showing lower conformational selectivity for the native wtTAR GS as compared to ARG and DMA-169 (Fig 3b).

In conclusion, our study shows that structure-specific drug-like small molecules can bind and stabilize low-abundance short-lived ES conformations of RNA. That ARG and DMA-169 can bind and stabilize the ES of $TAR^{UUCG\text{-}ES}$ while showing no evidence for binding to the more abundant GS structure, suggests that these molecules achieve a significant conformational specificity, especially considering that the RNA sequence is unchanged. Future studies should examine how the abundance of the ES and the kinetics of GS-ES inter-conversion affect the thermodynamics and kinetics of small molecule binding and to test the expectation that binding is slower and weaker in a manner dependent on the ES lifetime and population, respectively. Since many ES conformations are likely to be inactive based on their altered base pairing, these results support the feasibility of specifically stabilizing RNA excited states as a therapeutic strategy. However, because the population of the $TAR^{UUCG\text{-}ES}$ ES (~12%) is about 30-fold higher than the ES population of wtTAR (0.4%), targeting the inactive ES of wtTAR will require correspondingly higher binding selectivity to shift the conformational equilibrium by a similar amount. The $TAR^{UUCG\text{-}ES}$ mutant offers a useful model system for studying small molecule recognition of RNA ESs.

Materials and Methods

Predicted secondary structure

The program MC-Fold [37] was used to predict RNA secondary structures. Compared to other programs, MC-Fold assigns lower energies to mismatches, which we find agrees better with our non-canonical excited states.

RNA sample preparation

$^{13}C/^{15}N$ labeled RNA samples (G/A-type, U-type, and C-type labeled $TAR^{UUCG\text{-}ES}$, as well as uniformly labeled $TAR^{UUCG\text{-}ES}$) were prepared by *in vitro* transcription using T7 RNA polymerase (New England BioLabs), DNA template (Integrated DNA Technologies) containing the T7 promoter, and labeled $13C/^{15}N$- labeled nucleotide triphosphates (Cambridge Isotope Laboratories, Inc.). The transcription reaction was carried out at 37 °C for 12 hours and then filtered with a 0.2 μm filter. Samples were purified using a 20% (w/v) polyacrylamide gel with 8 M urea and 1 × Tris/borate/EDTA. The RNA was removed from the excised gel by electro-elution in 1× Tris/acetic acid/EDTA followed by ethanol precipitation. The RNA was annealed in water at a concentration of 50 μM by heating at 95 °C for 5 min followed by cooling on ice for 30 min. The RNA was then buffer exchanged using an Amicon Ultra-15 centrifugal filter (EMD Millipore) with a 3 kDa cutoff into NMR buffer [15 mM sodium phosphate, 25 mM sodium chloride, 0.1 mM EDTA at pH 6.4]. Samples contained either 10% or 100% (v/v) D_2O (after lyophlization) as indicated below. The final concentration of RNA in all samples was approximately 1 mM.

Small molecule preparation

L-argininamide dihydrochloride (Sigma) and Neomycin trisulfate salt hydrate (Sigma) were purchased in powder form and dissolved in NMR buffer before being added to the RNA sample. DMA derivative 24 was obtained as described previously[2] and was stored at 50 mM in 100% dimethyl sulfoxide (DMSO).

NMR spectroscopy

All NMR experiments were carried out at 25°C on a 6 00 MHz Bruker Avance III spectrometer equipped with HCN cryogenic probes.

^{13}C $R_{1\rho}$ relaxation dispersion

Off-resonance ^{13}C $R_{1\rho}$ relaxation dispersion (RD) NMR experiments were carried out on G/A-, U-type, and C-type $^{13}C/^{15}N$-labeled $TAR^{UUCG\text{-}ES}$ samples in NMR buffer with 100% (v/v) D_2O. On- and off-resonance $R_{1\rho}$ RD profiles for C6/C8/C1' spins were measured using a 1D acquisition scheme [48] with spinlock powers ($\omega 2\pi^{-1}$ Hz) and offsets ($\Omega 2\pi^{-1}$ Hz) listed in Supplementary Table 1 and using nine time delay points. For each delay time point, peak intensities were obtained using NMRPipe [49] and $R_{1\rho}$ values were calculated by fitting to a monoexponential decay function using an in-house python script[5]. Errors in $R_{1\rho}$ were estimated using Monte Carlo simulations with 500 iterations as previously described [31, 50]. The RD data was analyzed to obtain exchange parameters through numerical solutions of the Bloch-McConnell equations [51] using an in-house python script [31, 52]. Data was fit individually and globally to a two-state model using automatic effective field alignment. Model selection was preformed as previously described [31] using the Akaike's (ω_{AIC}) and Bayesian information criterion (w_{BIC}) weights to select the model with the highest relative probability. Fitting with and without G54-C1' resulted in parameters that were within error, so we opted to include it despite it being noisy.

NMR chemical shift mapping

Resonance assignments were obtained from prior studies of wtTAR [53] UUCG-ES TAR [27], UUCG-GS TAR [53], UUCG-ES+ARG [26], UUCG-GS TAR+neomycin [26]. NMR chemical shift mapping experiments were preformed by recording 2D [^{13}C-^{1}H] SOFAST-HMQC NMR experiments [39] on 50 μM uniformly labeled RNA samples (wtTAR, $TAR^{UUCG\text{-}ES}$, and $TAR^{UUCG\text{-}GS}$) in NMR buffer with 10% (v/v) D_2O following incremental addition of the small molecule. Data were processed using NMRpipe [49] and analyzed using SPARKY [54].

Supplementary Material

Refer to Web version on PubMed Central for supplementary material.

Acknowledgements

We would like to thank the Duke Magnetic Resonance Spectroscopy Center for NMR resources. This work was supported by the US National Institutes of Health (P50 GM103297 to H.M.A.-H and F31 GM119306 to L.R.G).

Abbreviations

ES	excited conformational state
GS	ground state
TAR	transactivation response element
RRE	Rev response element
wtTAR	wild-type TAR
RD	relaxation dispersion
ARG	argininamide

References

[1]. Donlic A, Hargrove AE. Targeting RNA in mammalian systems with small molecules. Wiley interdisciplinary reviews RNA. 2018;9:e1477. [PubMed: 29726113]

[2]. Connelly CM, Moon MH, Schneekloth JS Jr. The emerging role of RNA as a therapeutic target for small molecules. Cell chemical biology. 2016;23:1077–90. [PubMed: 27593111]

[3]. Shortridge MD, Varani G. Structure based approaches for targeting non-coding RNAs with small molecules. Current opinion in structural biology. 2015;30:79–88. [PubMed: 25687935]

[4]. Matsui M, Corey DR. Non-coding RNAs as drug targets. Nature reviews Drug discovery. 2017;16:167–179. [PubMed: 27444227]

[5]. Di Giorgio A, Duca M. Synthetic small-molecule RNA ligands: future prospects as therapeutic agents. MedChemComm. 2019;10:1242–55. [PubMed: 31534649]

[6]. Hermann T. Rational ligand design for RNA: the role of static structure and conformational flexibility in target recognition. Biochimie. 2002;84:869–75. [PubMed: 12458079]

[7]. Hermann T. Small molecules targeting viral RNA. Wiley interdisciplinary reviews RNA. 2016;7:726–43. [PubMed: 27307213]

[8]. Fourmy D, Recht MI, Blanchard SC, Puglisi JD. Structure of the A site of Escherichia coli 16S ribosomal RNA complexed with an aminoglycoside antibiotic. Science. 1996;274:1367–71. [PubMed: 8910275]

[9]. Carter AP, Clemons WM, Brodersen DE, Morgan-Warren RJ, Wimberly BT, Ramakrishnan V. Functional insights from the structure of the 30S ribosomal subunit and its interactions with antibiotics. Nature. 2000;407:340–8. [PubMed: 11014183]

[10]. Chavali SS, Bonn-Breach R, Wedekind JE. Face-time with TAR: Portraits of an HIV-1 RNA with diverse modes of effector recognition relevant for drug discovery. J Biol Chem. 2019;294:9326–9341. [PubMed: 31080171]

[11]. Shortridge MD, Wille PT, Jones AN, Davidson A, Bogdanovic J, Arts E, et al. An ultra-high affinity ligand of HIV-1 TAR reveals the RNA structure recognized by P-TEFb. Nucleic acids research. 2019;47:1523–31. [PubMed: 30481318]

[12]. Dethoff EA, Petzold K, Chugh J, Casiano-Negroni A, Al-Hashimi HM. Visualizing transient low-populated structures of RNA. Nature. 2012;491:724–8. [PubMed: 23041928]

[13]. Lee J, Dethoff EA, Al-Hashimi HM. Invisible RNA state dynamically couples distant motifs. Proceedings of the National Academy of Sciences of the United States of America. 2014;111:9485–90. [PubMed: 24979799]

[14]. Blad H, Reiter NJ, Abildgaard F, Markley JL, Butcher SE. Dynamics and metal ion binding in the U6 RNA intramolecular stem-loop as analyzed by NMR. Journal of molecular biology. 2005;353:540–55. [PubMed: 16181635]

[15]. Hoogstraten CG, Wank JR, Pardi A. Active site dynamics in the lead-dependent ribozyme. Biochemistry. 2000;39:9951–8. [PubMed: 10933815]

[16]. Xue Y, Gracia B, Herschlag D, Russell R, Al-Hashimi HM. Visualizing the formation of an RNA folding intermediate through a fast highly modular secondary structure switch. Nature communications. 2016;7:ncomms11768.

[17]. Chen B, LeBlanc R, Dayie TK. SAM-II riboswitch samples at least two conformations in solution in the absence of ligand: Implications for recognition. Angewandte Chemie (International ed in English). 2016;55:2724–7. [PubMed: 26800479]

[18]. Zhao B, Guffy SL, Williams B, Zhang Q. An excited state underlies gene regulation of a transcriptional riboswitch. Nature chemical biology. 2017;13:968–74. [PubMed: 28719589]

[19]. Weeks KM, Ampe C, Schultz SC, Steitz TA, Crothers DM. Fragments of the HIV-1 Tat protein specifically bind TAR RNA. Science. 1990;249:1281–5. [PubMed: 2205002]

[20]. Frankel AD. Activation of HIV transcription by Tat. Curr Opin Genet Dev. 1992;2:293–8. [PubMed: 1638124]

[21]. Malim MH, Hauber J, Le SY, Maizel JV, Cullen BR. The HIV-1 rev trans-activator acts through a structured target sequence to activate nuclear export of unspliced viral mRNA. Nature. 1989;338:254–7. [PubMed: 2784194]

[22]. Chu CC, Plangger R, Kreutz C, Al-Hashimi HM. Dynamic ensemble of HIV-1 RRE stem IIB reveals non-native conformations that disrupt the Rev-binding site. Nucleic acids research. 2019;47:7105–17. [PubMed: 31199872]

[23]. Ganser LR, Chu CC, Bogerd HP, Kelly ML, Cullen BR, Al-Hashimi HM. Probing RNA conformational equilibria within the functional cellular context. bioRXiv. 2019. doi: 10.1101/634576.

[24]. Puglisi JD, Tan R, Calnan BJ, Frankel AD, Williamson JR. Conformation of the TAR RNA-arginine complex by NMR spectroscopy. Science. 1992;257:76–80. [PubMed: 1621097]

[25]. Aboul-ela F, Karn J, Varani G. Structure of HIV-1 TAR RNA in the absence of ligands reveals a novel conformation of the trinucleotide bulge. Nucleic acids research. 1996;24:3974–81. [PubMed: 8918800]

[26]. Stelzer AC, Kratz JD, Zhang Q, Al-Hashimi HM. RNA Dynamics by design: Biasing ensembles towards the ligand-bound state. Angewandte Chemie (International ed in English). 2010; 49:5731–3. [PubMed: 20583015]

[27]. Clay MC, Ganser LR, Merriman DK, Al-Hashimi HM. Resolving sugar puckers in RNA excited states exposes slow modes of repuckering dynamics. Nucleic acids research. 2017;45:e134. [PubMed: 28609788]

[28]. Abulwerdi FA, Le Grice SFJ. Recent advances in targeting the HIV-1 Tat/TAR complex. Current pharmaceutical design. 2017;23:4112–21. [PubMed: 28625133]

[29]. Ganser LR, Lee J, Rangadurai A, Merriman DK, Kelly ML, Kansal AD, et al. High-performance virtual screening by targeting a high-resolution RNA dynamic ensemble. Nature structural & molecular biology. 2018;25:425–34.

[30]. Merriman DK, Xue Y, Yang S, Kimsey IJ, Shakya A, Clay M, et al. Shortening the HIV-1 TAR RNA bulge by a single nucleotide preserves motional modes over a broad range of time scales. Biochemistry. 2016;55:4445–56. [PubMed: 27232530]

[31]. Rangadurai A, Szymaski ES, Kimsey IJ, Shi H, Al-Hashimi HM. Characterizing micro-to-millisecond chemical exchange in nucleic acids using off-resonance R1rho relaxation dispersion. Progress in nuclear magnetic resonance spectroscopy. 2019;112–113:55–102.

[32]. Hansen AL, Nikolova EN, Casiano-Negroni A, Al-Hashimi HM. Extending the range of microsecond-to-millisecond chemical exchange detected in labeled and unlabeled nucleic acids by selective carbon R(1rho) NMR spectroscopy. Journal of the American Chemical Society. 2009;131:3818–9. [PubMed: 19243182]

[33]. Palmer AG, 3rd. Chemical exchange in biomacromolecules: Past, present, and future. Journal of magnetic resonance. 2014;241:3–17. [PubMed: 24656076]

[34]. Sekhar A, Kay LE. NMR paves the way for atomic level descriptions of sparsely populated, transiently formed biomolecular conformers. Proceedings of the National Academy of Sciences of the United States of America. 2013; 110:12867–74. [PubMed: 23868852]

[35]. Bouvignies G, Vallurupalli P, Hansen DF, Correia BE, Lange O, Bah A, et al. Solution structure of a minor and transiently formed state of a T4 lysozyme mutant. Nature. 2011;477:111–4. [PubMed: 21857680]

[36]. Nikolova EN, Kim E, Wise AA, O'Brien PJ, Andricioaei I, Al-Hashimi HM. Transient Hoogsteen base pairs in canonical duplex DNA. Nature. 2011;470:498–502. [PubMed: 21270796]

[37]. Parisien M, Major F. The MC-Fold and MC-Sym pipeline infers RNA structure from sequence data. Nature. 2008;452:51–5. [PubMed: 18322526]

[38]. Salmon L, Giambaşu GM, Nikolova EN, Petzold K, Bhattacharya A, Case DA, et al. Modulating RNA alignment using directional dynamic kinks: Application in determining an atomic-resolution ensemble for a hairpin using NMR residual dipolar couplings. Journal of the American Chemical Society. 2015;137:12954–65. [PubMed: 26306428]

[39]. Sathyamoorthy B, Lee J, Kimsey I, Ganser LR, Al-Hashimi H. Development and application of aromatic [(13)C, (1)H] SOFAST-HMQC NMR experiment for nucleic acids. Journal of biomolecular NMR. 2014;60:77–83. [PubMed: 25186910]

[40]. Salmon L, Yang S, Al-Hashimi HM. Advances in the determination of nucleic acid conformational ensembles. Annual review of physical chemistry. 2014;65:293–316.

[41]. Ganser LR, Kelly ML, Herschlag D, Al-Hashimi HM. The roles of structural dynamics in the cellular functions of RNAs. Nature Reviews Molecular Cell Biology. 2019;20:474–89. [PubMed: 31182864]

[42]. Pitt SW, Majumdar A, Serganov A, Patel DJ, Al-Hashimi HM. Argininamide binding arrests global motions in HIV-1 TAR RNA: comparison with Mg2+-induced conformational stabilization. Journal of molecular biology. 2004;338:7–16. [PubMed: 15050819]

[43]. Latham MP, Zimmermann GR, Pardi A. NMR chemical exchange as a probe for ligand-binding kinetics in a theophylline-binding RNA aptamer. Journal of the American Chemical Society. 2009;131:5052–3. [PubMed: 19317486]

[44]. Patwardhan NN, Ganser LR, Kapral GJ, Eubanks CS, Lee J, Sathyamoorthy B, et al. Amiloride as a new RNA-binding scaffold with activity against HIV-1 TAR. MedChemComm. 2017;8:1022–36. [PubMed: 28798862]

[45]. Faber C, Sticht H, Schweimer K, Rösch P. Structural rearrangements of HIV-1 Tat-responsive RNA upon binding of neomycin B. J Biol Chem. 2000;275:20660–6. [PubMed: 10747964]

[46]. Blount KF, Tor Y. Using pyrene-labeled HIV-1 TAR to measure RNA-small molecule binding. Nucleic Acids Research. 2003;31:5490–500. [PubMed: 14500811]

[47]. Bailor MH, Sun X, Al-Hashimi HM. Topology links RNA secondary structure with global conformation, dynamics, and adaptation. Science. 2010;327:202–6. [PubMed: 20056889]

[48]. Nikolova EN, Gottardo FL, Al-Hashimi HM. Probing transient Hoogsteen hydrogen bonds in canonical duplex DNA using NMR relaxation dispersion and single-atom substitution. JACS. 2012;134:3667–70.

[49]. Delaglio F, Grzesiek S, Vuister GW, Zhu G, Pfeifer J, Bax A. NMRPipe: a multidimensional spectral processing system based on Unix pipes. Journal of Biomolecular NMR. 1995;6:277–93. [PubMed: 8520220]

[50]. Bothe JR, Stein ZW, Al-Hashimi HM. Evaluating the uncertainty in exchange parameters determined from off-resonance R1ρ relaxation dispersion for systems in fast exchange. Journal of Magnetic Resonance. 2014;244:18–29. [PubMed: 24819426]

[51]. McConnell HM. Reaction rates by nuclear magnetic resonance. J Chem Phys. 1958;28:430–1.

[52]. Kimsey IJ, Petzold K, Sathyamoorthy B, Stein ZW, Al-Hashimi HM. Visualizing transient Watson-Crick-like mispairs in DNA and RNA duplexes. Nature. 2015;519:315–20. [PubMed: 25762137]

[53]. Dethoff EA, Hansen AL, Musselman C, Watt ED, Andricioaei I, Al-Hashimi HM. Characterizing complex dynamics in the transactivation response element apical loop and motional correlations with the bulge by NMR, molecular dynamics, and mutagenesis. Biophysical journal. 2008;95:3906–15. [PubMed: 18621815]

[54]. Goddard TD, Kneller DG. SPARKY 3: University of California, San Franscisco.

Highlights

- Stabilizing low-abundance, short-lived RNA excited conformational states that have altered secondary structures is a promising approach for inhibiting RNA activity.
- Two small molecules that bind structures specific to the ground state conformation of HIV-1 TAR are shown to bind to the transiently formed low abundance ground state-like conformation in an HIV-1 TAR mutant that inverts the ground and excited state populations.
- An aminoglycoside that binds RNAs non-specifically is shown to bind to the TAR mutant without preferentially stabilizing the excited state.
- The results support the feasibility of inhibiting RNA activity using small molecules that preferentially bind and stabilize low-abundance and short-lived RNA excited conformational states.

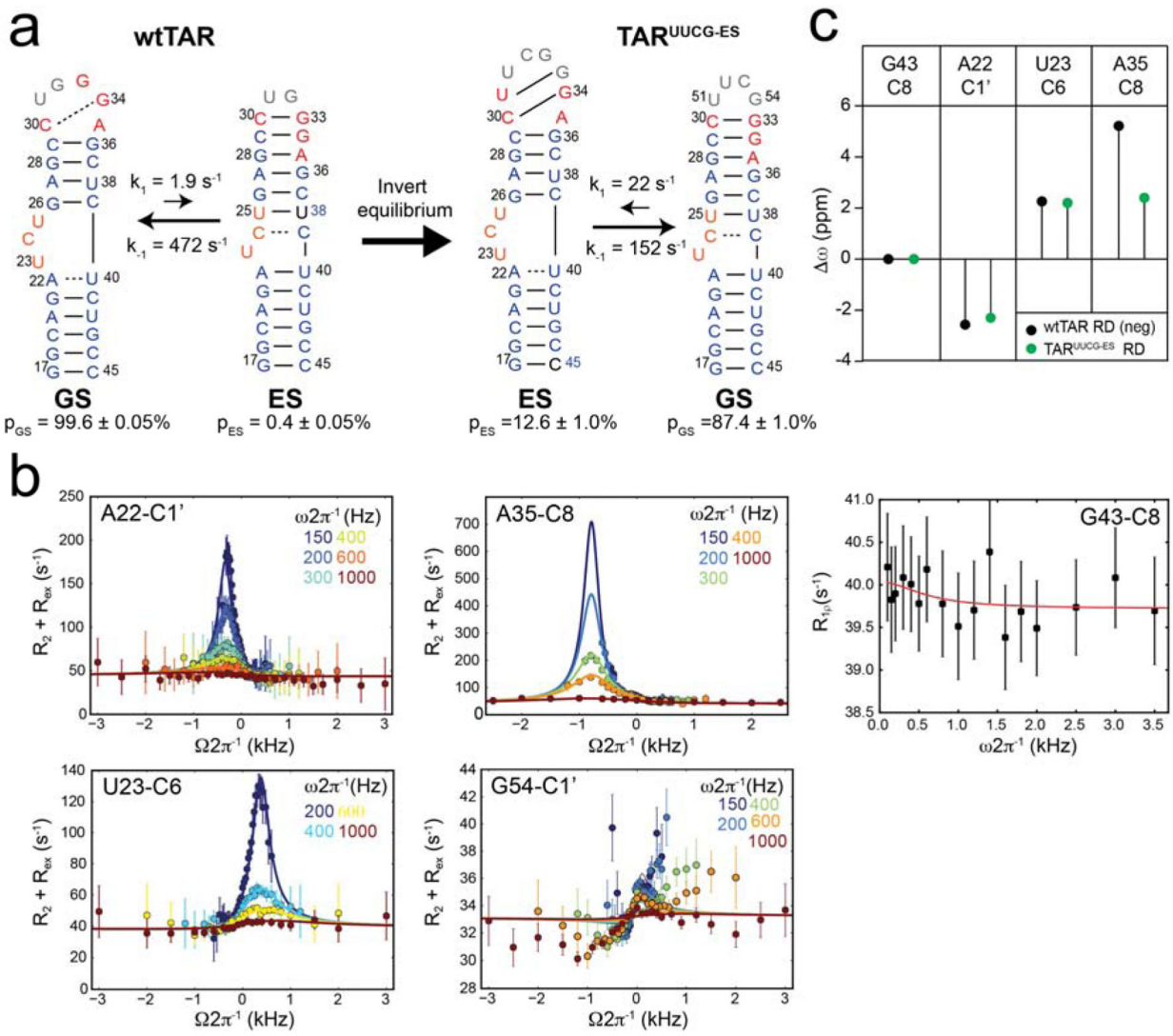

Figure 1.

The ES-stabilizing mutant TAR$^{UUCG-ES}$ experiences back exchange with a low-abundance and short-lived ES that has conformational features similar to the GS of wild-type TAR. **a**. Chemical exchange between the GS and ES in wtTAR and TAR$^{UUCG-ES}$. Shown are the populations (p_{GS} and p_{ES}) of the GS and ES, respectively and the rate constants (k_1 and k_{-1}) for inter-conversion deduced from 2-state analysis of the $R_{1\rho}$ RD data. Residues are labeled according to the wtTAR GS secondary structure: stem (blue), bulge (orange), apical loop (red). Residues that differ between the two TAR variants are in gray. **b**. $R_{1\rho}$ RD profiles measured for TAR$^{UUCG-ES}$. Off-resonance profiles show the dependence of $R_2 + R_{ex}$ on spinlock power ($\omega 2\pi^{-1}$) and offset ($\Omega 2\pi^{-1}$). Shown are the global fits (solid line) to a two-state model using the Bloch-McConnell equations assuming a two-state exchange process (Methods). On-resonance profiles show the dependence of $R_{1\rho}$ on spinlock power ($\omega 2\pi^{-1}$). Error bars represent experimental error determined by propagation of error determined by Monte Carlo analysis of monoexponential decay curves and experimental signal to noise. Data was collected on a 600 MHz (^{1}H frequency) spectrometer. Buffer conditions are 15

mM sodium phosphate, 25 mM sodium chloride, 0.1 mM EDTA, 100% D_2O at pH 6.4 and 25 °C. **c**. Comparison of the difference between chemical shifts measured for the ES and GS ($\Delta\omega = \omega_{ES} - \omega_{GS}$) in $TAR^{UUCG\text{-}ES}$ (green) and the inverse ($\Delta\omega = \omega_{GS} - \omega_{ES}$) in wtTAR (black) [13] using $R_{1\rho}$ RD NMR.

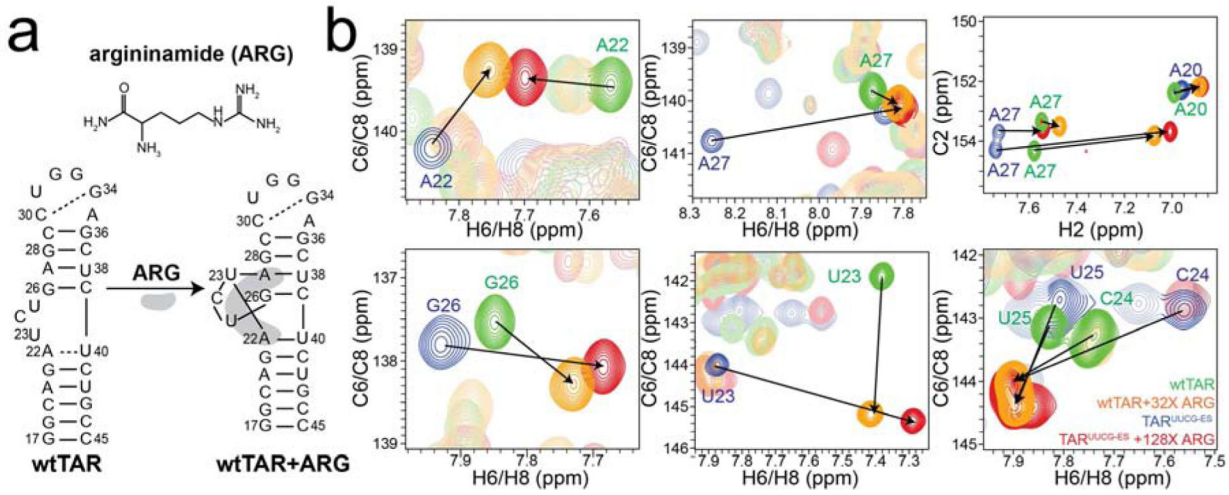

Figure 2.

Argininamide (ARG) binds and stabilizes the ES of $TAR^{UUCG\text{-}ES}$. a. ARG binds the wtTAR GS secondary structure and stabilizes a unique base triple conformation. b. 2D [^{13}C,^{1}H] aromatic SOFAST-HMQC [39] spectra of free $TAR^{UUCG\text{-}ES}$ (blue), $TAR^{UUCG\text{-}ES}$ + 128x ARG (red), free wtTAR (green), and wtTAR + 32x ARG (orange). Buffer conditions are 15 mM sodium phosphate, 25 mM sodium chloride, 0.1 mM EDTA, 10% D_2O at pH 6.4 and 25 °C.

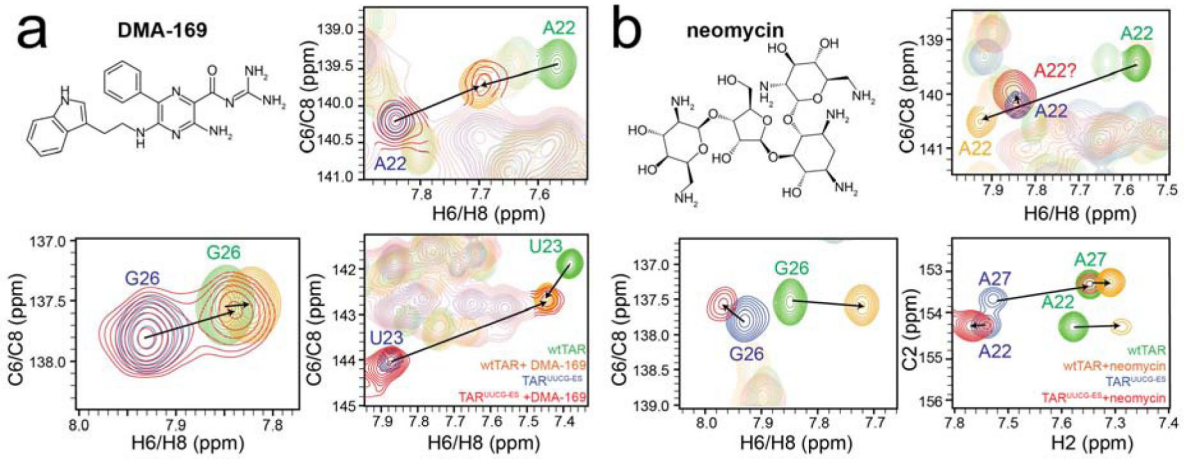

Figure 3.

Small molecules can partially stabilize or non-specifically bind RNA. 2D [^{13}C,^{1}H] aromatic SOFAST-HMQC [39] spectra of free TAR$^{UUCG-ES}$ (blue), TAR$^{UUCG-ES}$ + 16x small molecule (red), free wtTAR (green), and wtTAR + 8x small molecule (orange) for a. DMA-169 and b. neomycin. Buffer conditions are 15 mM sodium phosphate, 25 mM sodium chloride, 0.1 mM EDTA, 10% D_2O at pH 6.4 and 25 °C.